


Research Article

Oral Delivery of TDCA Attenuates Cognitive Decline and Amyloid Pathology in Alzheimer's Disease Model.

Md Jahirul Islam^{a,b,c}, Ju-yong Kim,^c Young-jae Koh,^c Seung-Yong Seong^{a,b,c,d*}

Abstract

Alzheimer's disease (AD) is characterized by cognitive impairment, amyloid-beta (A β) plaque accumulation, and neuroinflammation, with current treatments offering limited efficacy in altering disease progression. This study investigates the therapeutic potential of taurodeoxycholic acid (TDCA), a secondary bile acid with anti-inflammatory properties, as an orally administered treatment for AD.

In a 10-week study, TDCA was orally administered to 5xFAD transgenic mice, a model of familial AD, at a dose optimized for therapeutic benefit. Cognitive performance was evaluated using Morris Water Maze (MWM) and Novel Object Recognition (NOR) tests, while amyloid plaque deposition and neuronal integrity were assessed through Thioflavin-S staining and NeuN immunostaining, respectively.

TDCA-treated 5xFAD mice demonstrated significant improvements in spatial learning and memory in MWM and NOR tests compared to vehicle-treated controls. Treatment also resulted in a notable reduction in A β plaque burden, preserved NeuN-positive neurons, and decreased markers of neuroinflammation. By modulating microglial activity and suppressing the NLRP3 inflammasome, TDCA reduced pro-inflammatory cytokine secretion (IL-1 β , IL-18) and enhanced A β clearance via restored scavenger receptor A (SRA) expression. These findings highlight TDCA as a promising oral therapeutic candidate for AD, capable of attenuating cognitive decline and amyloid pathology while targeting key neuroinflammatory mechanisms.

Keywords: Taurodeoxycholate; Alzheimer's disease; Neuroinflammation; Microglia; Inflammasome.

Introduction

Alzheimer's disease (AD) is a progressive neurodegenerative disorder characterized by the accumulation of amyloid-beta (A β) plaques and neurofibrillary tangles, leading to cognitive decline and memory loss[1]. Despite extensive research, effective treatments that can halt or reverse the progression of AD remain elusive. FDA-approved treatments for AD, such as cholinesterase inhibitors (e.g., donepezil)[2] and NMDA receptor antagonists (e.g., memantine)[3], primarily offer symptomatic relief without addressing the underlying disease mechanisms[4]. These treatments, while beneficial in managing symptoms, do not significantly alter the course of the disease. In recent years, anti-amyloid treatments, such as monoclonal antibodies targeting A β plaques, have been developed and received FDA approval[5]. Notable examples include aducanumab and lecanemab[6], which aim to reduce A β plaque accumulation in the brain, potentially slowing the progression of

Affiliation:

^aWide River Institute of Immunology, Seoul National University College of Medicine, Seoul, Republic of Korea

^bDepartment of Biomedical Sciences, Seoul National University College of Medicine, Seoul, Republic of Korea

^cShaperon Inc. Ltd, Seoul, Republic of Korea

^dDepartment of Microbiology and Immunology, Seoul National University College of Medicine, Seoul, Republic of Korea

*Corresponding author:

Seung-Yong Seong, Department of Microbiology and Immunology Wide River Institute of Immunology, Seoul National University College of Medicine 103 Daehakno, Jongno-gu, Seoul, South Korea.

Citation: Md Jahirul Islam, Ju-yong Kim, Young-jae Koh, Seung-Yong Seong. Oral Delivery of TDCA Attenuates Cognitive Decline and Amyloid Pathology in Alzheimer's Disease Model. *Journal of Psychiatry and Psychiatric Disorders*. 9 (2025): 50-61.

Received: January 22, 2025

Accepted: February 03, 2025

Published: February 13, 2025

AD[7]. However, these treatments come with significant challenges, including high costs, limited accessibility, and the need for intravenous administration. The financial burden of these therapies, coupled with their invasive nature, has raised concerns about their long-term feasibility and widespread adoption.

A promising therapeutic strategy for AD involves targeting the inflammatory processes in the brain, particularly those mediated by microglia, the brain's resident immune cells[8]. Microglia play a central role in the brain's immune response and are crucial in maintaining homeostasis by clearing debris, including A β plaques[9]. However, in AD, chronic activation of microglia leads to a sustained inflammatory response that exacerbates neuronal damage and contributes to disease progression[10]. Targeting microglial activation and modulating their inflammatory responses have thus emerged as key strategies for treating AD. Central to this inflammatory response is the NLRP3 inflammasome, a multiprotein complex within microglia that senses pathogenic stimuli and triggers the release of pro-inflammatory cytokines, particularly interleukin-1 β (IL-1 β) and interleukin-18 (IL-18)[11]. In AD, activation of the NLRP3 inflammasome by A β leads to the secretion of IL-1 β and IL-18, which further amplify neuroinflammation and promote neuronal damage[12]. Targeting the NLRP3 inflammasome and its downstream effects on IL-1 β and IL-18 secretion has thus become a critical focus in developing therapies aimed at mitigating AD's progression. The relevance of the NLRP3 inflammasome extends beyond AD, as it plays a pivotal role in various chronic inflammatory and neurodegenerative diseases. Conditions such as Parkinson's disease, multiple sclerosis, and amyotrophic lateral sclerosis (ALS) have also been linked to dysregulated microglial activation and chronic neuroinflammation mediated by the NLRP3 inflammasome [13]. In these diseases, the persistent activation of the NLRP3 inflammasome contributes to the release of pro-inflammatory cytokines, which drive neurodegeneration and exacerbate disease symptoms. Thus, the NLRP3 inflammasome is increasingly recognized as a therapeutic target not only for AD but also for a broader range of inflammatory and neurodegenerative disorders.

Bile acid has recently gained attention as a potential therapeutic agent due to its anti-inflammatory and neuroprotective properties [14]. Bile acids, traditionally recognized for their roles in lipid digestion and cholesterol metabolism, are now being explored for their effects on the central nervous system (CNS)[15]. Taurodeoxycholic acid (TDCA) has been shown to modulate microglial activity and inhibit the activation of the NLRP3 inflammasome, thereby reducing the secretion of IL-1 β and IL-18, which are pivotal in the pathogenesis of AD. Our previous studies have demonstrated that intraperitoneal (i.p.) administration

of TDCA can improve cognitive function in animal models of AD, such as 5xFAD mice and exhibit accelerated A β deposition and neuroinflammation[16]. In these models, TDCA treatment has been shown to reduce the burden of A β plaques, decrease neuronal apoptosis, and modulate the action of purinergic ion channel (P2X7) receptor by binding to G protein couple receptor 19 (GPCR19). Modulation of P2X7R controls cellular Ca²⁺ and NLRP3 inflammasome[17, 18]. The therapeutic potential of TDCA in AD is further supported by behavioral studies showing that TDCA treatment leads to significant improvements in spatial learning and memory, as assessed by the Morris water maze (MWM) and Y-maze tests. These cognitive benefits, coupled with the reduction in A β plaques, neuroinflammation, and the inhibition of NLRP3-mediated IL-1 β and IL-18 secretion, suggest that TDCA could be a promising candidate for AD treatment[16]. In this study TDCA has been found to restore the expression of scavenger receptor A (SRA), a receptor involved in the clearance of A β by microglia, thereby enhancing the brain's ability to clear toxic amyloid aggregates[19]. In addition, TDCA's oral administration offers a more convenient and potentially less costly treatment option compared to anti-amyloid therapies such as aducanumab or symptomatic treatment. The high costs and invasive administration methods associated with anti-amyloid treatments limit their accessibility and long-term sustainability. In contrast, TDCA's non-invasive nature, combined with its multifaceted effects on microglial function, neuroinflammation, A β clearance, and neuronal survival, positions it as a novel and potentially effective treatment for AD.

Given the crucial role of microglia in driving inflammation and contributing to the progression of AD, particularly through the NLRP3 inflammasome and the downstream secretion of IL-1 β and IL-18, targeting these pathways with TDCA represents a compelling therapeutic approach. By modulating the inflammatory pathways mediated by microglia and inhibiting the NLRP3 inflammasome, TDCA not only addresses a core pathological feature of AD but also offers a more comprehensive strategy to mitigate the neurodegenerative processes underlying the disease. This approach warrants further investigation in both preclinical and clinical studies to validate its efficacy and safety in humans, potentially providing a more accessible and cost-effective therapeutic option for patients with AD and other chronic inflammatory neurodegenerative diseases.

Materials and Methods

Reagents

Taurodeoxycholic acid (TDCA) was sourced from New Zealand Pharmaceuticals Ltd. (Palmerston North, New Zealand). Adenosine triphosphate (ATP) was obtained from Sigma-Aldrich (St. Louis, MO, USA) and dissolved in phosphate-buffered saline (PBS).

Preparation of A β 1-42 Oligomer

A lyophilized vial containing 0.1 mg of amyloid beta protein fragments 1-42 (A β ; Sigma-Aldrich) was dissolved in 50 μ L of dimethyl sulfoxide (DMSO; Sigma-Aldrich) and incubated for 1 hour at room temperature with continuous rotation. The dissolved A β was then diluted to 100 μ M with DMEM or EMEM media and incubated at 4°C for 24 hours with continuous rotation to form oligomeric A β 1-42.

Cell Culture

BV2 cells (mouse microglial cell line) were cultured in Dulbecco's Modified Eagle's Medium (DMEM; Invitrogen, Carlsbad, CA, USA). HMC3 cells (human microglial cell line) were maintained in Eagle's Minimum Essential Medium (EMEM; ATCC, Cat no: 30-2003, USA). Both cell lines were grown in a 95% air and 5% CO₂ atmosphere at 37°C, supplemented with 10% fetal bovine serum (FBS; Invitrogen) and 1% penicillin-streptomycin (Invitrogen). Cells were seeded in poly-D-lysine (PDL)-coated 6-well (1.5 x 10⁵ cells/2 ml), 12-well (1 x 10⁵ cells/ml), or 24-well (5 x 10⁴ cells/0.5 ml) plates. Treatments included A β (2 μ M), TDCA (400 ng/ml) for 24 hours, and ATP (1 mM) for the final hour. Supernatants from these cultures were collected for cytokine analysis using ELISA.

Immunocytochemistry

BV2 or HMC3 cells were seeded on 12-mm coverslips in 24-well plates and treated with A β (2 μ M), TDCA (400 ng/ml) for 24 hours, and ATP (1 mM) for the final hour. Cells were permeabilized and stained with primary antibodies: anti-NLRP3 (Abcam, Cambridge, UK) and anti-ASC (Clone B-3, Santa Cruz Biotechnology, Inc., Dallas, TX, USA) at 4°C overnight. This was followed by staining with secondary antibodies: Alexa Fluor 488-labeled goat anti-rabbit IgG or Alexa Fluor 532-labeled goat anti-mouse IgG (Invitrogen) for 1 hour at room temperature. HMC3 cells were also stained with anti-SRA antibody (Novus Biologicals) and secondary goat anti-rabbit IgG Alexa Fluor 488 (Thermo Fisher Scientific) for 1 hour at room temperature. Coverslips were mounted with DAPI mounting solution (Vector Laboratories, Burlingame, CA, USA) and visualized using a Nikon A1 confocal microscope. Image analysis for colocalization and mean fluorescence intensity (MFI) was performed using ImageJ software and NIS-Elements AR (version 4.2, Nikon).

Quantitative RT-PCR

Total RNA was extracted from treated cells using the RNeasy Plus Mini kit (QIAGEN, Hilden, Germany). Complementary DNA (cDNA) was synthesized from 1 μ g of total RNA using the Maxime RT PreMix kit (iNtRON Biotechnology, Gyeonggi-do, South Korea). Quantitative PCR (qPCR) was conducted using SYBR Green Fast mix (Applied Biosystems, Woolston, Warrington, UK) and gene-specific primers (Supplementary Table 2) on the StepOnePlus

Real-Time PCR system (Applied Biosystems, Singapore). Relative expression levels were calculated using the ddCt method and normalized to mouse GAPDH.

ELISA

Cytokine levels (IL-1 β and IL-18) in cell culture supernatants were quantified using ELISA kits for human IL-1 β (R&D Systems, Minneapolis, MN, USA) and IL-18 (MBL, Nagoya Aichi, Japan), following the manufacturer's protocols.

Animals

The 5xFAD mice co-overexpress high levels of APP with three FAD mutations (Swedish (K670N/M671L), Florida (I716V), and London (V717I)) and high levels of presenilin 1 (PSEN1) with two FAD mutations (M146L, L286V), which are specifically overexpressed in the brain and regulated by the neural-specific Thy1 promoter[20]. 5xFAD mice were maintained by breeding male 5xFAD mice with female B6 mice. The SJL F1 hybrid was produced by an SJL male and a

B6 female. PCR was performed to genotype the mice. 5xFAD or SJL mice were kindly provided by Professor Mook-Jung, In-hee or Professor Sung, Jung-Joon, respectively, of Seoul National University. All animal procedures were approved by the Seoul National University IACUC (SNU-170517-25) and followed ethical guidelines. Mice were housed in specific pathogen-free conditions at the Wide River Institute of Immunology.

In Vivo pharmacokinetic procedures

5xFAD mice were dosed via gavage needle for oral administration at 30 mg/kg (PO). Mice were sacrificed to harvest blood and brain samples at 2, 4, 8, 12, 24 and 48 h after dosing and processed for analysis. Blood plasma and brain samples were stored at -70°C until analysis for pharmacokinetic comparison. Indicated tissues were examined for TDCA content at the end of the study.

Bioanalysis of In Vivo pharmacokinetic samples

Plasma and brain bioanalysis samples were prepared based on previously published methods [21]. Briefly, three volumes of PBS buffer (pH 7.4) were added to one volume of each brain sample, then homogenized to obtain each brain homogenate sample. Three volumes of acetonitrile were added to one volume of plasma or brain tissue lysate to precipitate proteins. Samples were centrifuged (3000 g for 10 min) and supernatants removed for analysis by LC-MS/MS. Calibration standards and quality controls were made by preparation of a 1 mg/ml stock solution in methanol and subsequently a series of working solutions in methanol : water (1:1, v/v) which were spiked into blank plasma to yield a series of calibration standard samples in the range of 10 ng/ml to 10 μ g/ml and quality control samples at three concentration levels (low, middle, and high). All PK plasma

samples incurred were treated identically to the calibration standards and quality control samples. LC-MS/MS analysis was performed utilizing multiple reaction monitoring for detection of characteristic ions for each drug candidate, additional related analytes, and the internal standard

Morris water maze test:

Male and female 5xFAD mice (8 to 10 weeks old) were administered orally twice in a day (p.o, b.i.d) with either 30 mg/kg TDCA or PBS for 10 weeks. Age- and gender-matched nontransgenic littermates were used as a control group. Behavioral tests were performed after treatment, and then mice were sacrificed for further experimentation. The maze was composed of a circular pool (1.5 m in diameter, 80 cm in height) with spatial cues at three different locations. Before testing, the pool was filled with opaque water adjusted to $20 \pm 1^\circ\text{C}$. On the first day, mice were allowed to freely swim in the water for 60 sec to find the escape platform located in one quadrant of the pool. When the mice failed to find the platform, they were

guided to the platform. Once on the platform, mice were allowed to remain there for 30 sec. From the next day for 3 consecutive days, the same procedure was repeated from three different starting points to train the mouse, and the time to reach the platform was recorded every day. After the 4-day training period, the probe test was performed in the same manner but without the platform. Each mouse was allowed to swim from one starting point for 60 sec, which was recorded using a video camera. The video was analyzed for the movement of mice in the water using tracking software (SMART3.0, Panlab Harvard Apparatus, Barcelona, Spain) to count the number of crossings and the time on the platform and to measure the time spent in each quadrant of the pool.

Novel object recognition test (NORT):

NORT was assessed over the course of 4 days. The apparatus consisted of a white acrylic box (350 mm x 450 mm x 250 mm). The basement of the box was divided into six equal rectangles. On the first 2 days, each mouse was habituated to the box for 10 min. On the third day, two similar cylindrical objects were fixed in the box, and mice were allowed to explore the objects freely for 10 min. On the last day, one cylindrical object was replaced by a similarly sized object, and the mouse explored this for 5 min. Exploration of two cylindrical objects on the third day and exploration of the novel object and cylindrical object on day 4 were recorded for each mouse using a video camera. The total time and frequency of novel and old object exploration were counted for each mouse using the video footage. The percent discrimination index of the novel object was calculated from the exploration time of novel and old objects.

Immunohistochemistry

TDCA- or PBS-treated 5xFAD or B6 mice were

anesthetized and perfused with ice-cold PBS. Brains were harvested and maintained in 10% neutral buffer formalin (Sigma-Aldrich) for 24 h at 4°C and then embedded in paraffin (Lecia, Illinois, USA). The paraffin-embedded brains were cut ($3\ \mu\text{M}$) using microtome (Thermo Fisher Scientific), deparaffinized in xylene, and rehydrated in a graded ethanol series (100%, 90%, 80%, and 70%). Antigen unmasking was performed by heating the brain sections in a citrate-based buffer (pH 6, Vector laboratories, Burlingame, CA, USA). The sections were incubated in 0.3% Triton X-100 for 30 min at room temperature for intracellular staining and then blocked with a blocking solution of 10% normal goat serum (Thermo Fisher Scientific) and 1% BSA in PBS for 1 h. Tissue samples were incubated overnight at 4°C with NeuN (Clone A60, Merk Millipore, Temecula, CA, USA). Slices were subsequently incubated for 1 h at room temperature with Alexa 532-conjugated IgG secondary antibodies then counterstained with DAPI for 10 min. The A β core plaque was labeled by treating brain tissues with 1% thioflavin-S (Sigma-Aldrich) in PBS for 10 min at room temperature after being deparaffinized in xylene and rehydrated in a graded ethanol series (100%, 90%, 80%, and 70%). The tissue slides were then washed three times with 70% ethanol following DW three times. Fluorescence imaging was performed using a Confocal Microscope A1 (Nikon). NIS-Elements.AR. Ink (version 4.2, Nikon) was used to measure the MFI of the ROI.

Statistical analysis

The data are expressed as the mean \pm SEM and were analyzed using a two-sided, unpaired Student's t-test. The mean value between groups was compared using GraphPad Prism 5.0 software (GraphPad Software, La Jolla, CA, USA) unless otherwise indicated. P values < 0.05 were considered statistically significant.

Results

TDCA improves the spatial learning and memory of 5xFAD mice

A major consideration for the potential development of small molecules therapeutics for disorders is bioavailability, particularly in the brain. In this study, we used 5xFAD mice used for efficacy tests. TDCA PK studies are traditionally conducted using a single, acute dose paradigm. TDCA 100~500ng/ml was detected in mice plasma and Brain and start to decrease its concentration by 12h.

B6 and 5xFAD mice were administered with PBS or TDCA for 10 weeks (30 mg/kg, p.o, b.i.d), and spatial learning and memory were assessed using the Morris water maze (MWM) test (Supplementary Figure 1a). There were no significant changes in body weight after TDCA treatment for 10 weeks (Supplementary Figure 2b). Escape latency decreased over the 4-day training period in all three groups. Mice in the TDCA group showed a significant reduction in

time latency to reach the platform (Figure 1b), which was comparable to that of B6 mice. In the probe test on day 5, TDCA-treated 5xFAD mice showed increased numbers of platform crossings (Figure 1c). TDCA-treated 5xFAD mice remained for longer periods of time in the target quadrant than in the opposite quadrant compared with PBS-treated 5xFAD mice (Figure 1d). Times in the target quadrant and on the platform of 5xFAD-TDCA group were comparable to those of B6 mice. The mean speed (Supplementary Figure 1c) and total distance (Supplementary Figure 1d) traveled in the

MWM probe test is not significantly different between TDCA or PBS treated 5xFAD 286 and B6 mice.

Spatial learning and memory were also assessed using a novel object recognition test (NOR). In the NOR test, exploration time to a new object compared to an old object was significantly higher in B6-PBS and 5xFAD-TDCA mice. 5xFAD-PBS mice did not exhibit a difference in exploration time between old and new objects. The discrimination index for the mice in the 5xFAD-TDCA group was significantly higher than that for mice in the 5xFAD-PBS group (Figure 1e).

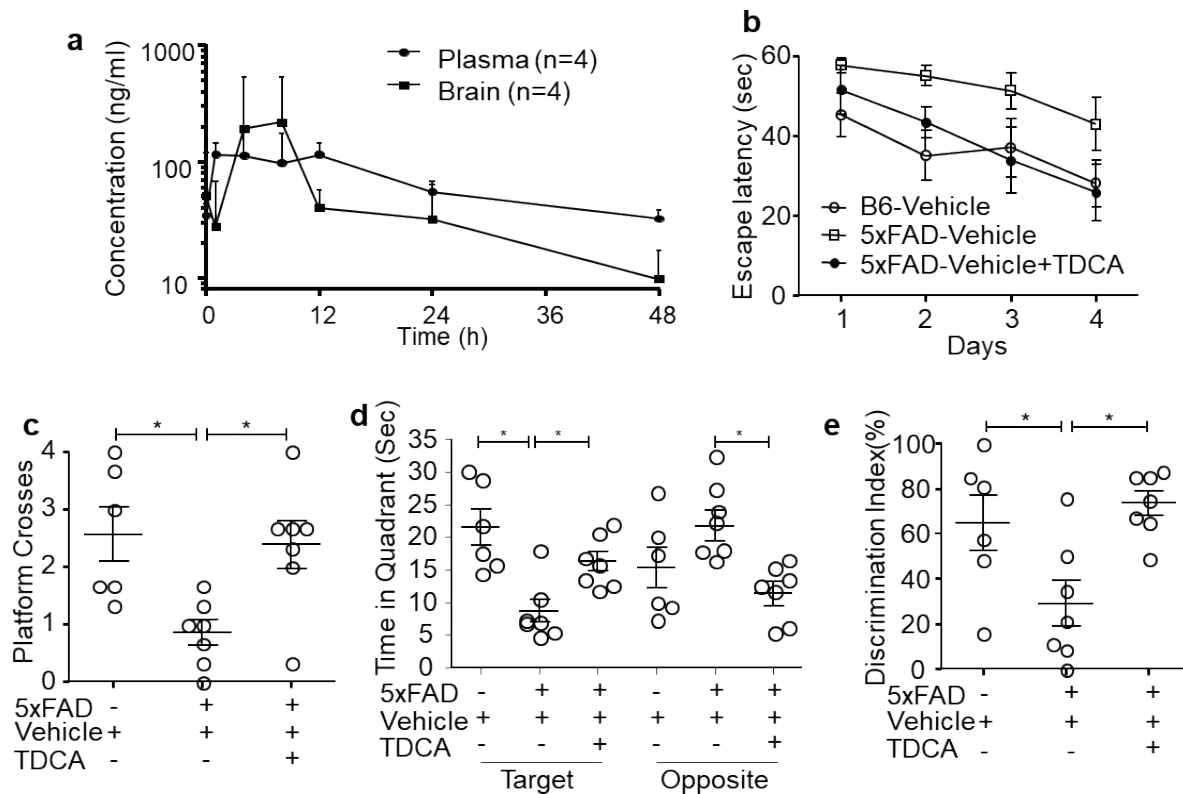


Figure 1: TDCA improves memory function in 5xFAD mice brain

a, PK profile of 30 mpk oral TDCA in B6 mice after a single administration was checked for different time points until 48 h. The learning and memory of 5xFAD and B6 (5xFAD) mice were tested after treatment with TDCA 30 mg/kg p.o. for 10 weeks (n = 6~7 / group). **b**, The time to reach the hidden platform (escape latency) **c**, the number of platform crosses and **d**, time staying in the target quadrant where a platform is located, and the opposite quadrant were measured using the MWM test. **e**, Discrimination index (%) = 100 × time spent exploring the novel object/exploration time for both the novel and old objects for each mouse (n = 10). The individual samples are shown with the mean ± SEM and *P < 0.05 using Student’s unpaired t- test throughout the study otherwise denoted.

TDCA decreases apoptosis of neurons and Aβ plaques in 5xFAD mouse brains

5xFAD mice brain slice was stained for Thio-S or NeuN after treatment with TDCA or PBS for 10 weeks (30 mg/kg, p.o, b.i.d). The numbers of Aβ plaques (white arrows) in the frontal cortex of 5xFAD mice decreased after TDCA treatment (Figure 1a, b) compared to PBS treatment. Then the number of NeuN+ cells in the frontal cortex were significantly higher in 5xFAD mice treated with TDCA than in those of 5xFAD mice treated with PBS (Figure 2c). NeuN staining

indicates healthy neurons which indicates less apoptotic cells after treatment with TDCA.

TDCA suppresses N3I activation of microglia by Aβ ± ATP

It was reported that Aβ (2.5~5 μM) could induce caspase-1-mediated IL-1β secretion by microglia[22]. In our setting HMC3 cells increased the production and secretion of IL-1β, and IL- 18 upon treatment with Aβ ± ATP, while TDCA suppressed the production of these cytokines (Figure 3a b). When HMC3 cells were treated with Aβ (2 μM) ± ATP

(1mM), the transcript levels of NLRP3, ASC, pro-caspase-1, and proIL-1 β were increased (Figure 3c d e and f). Although A β (2 μ M) alone could increase these transcripts, ATP

alone did not increase these transcript levels (but proIL-1 β), suggesting that A β (2 μ M) alone could activate priming phase of NLRP3 inflammasome. TDCA significantly inhibited the upregulation of these transcripts increased by A β \pm ATP.

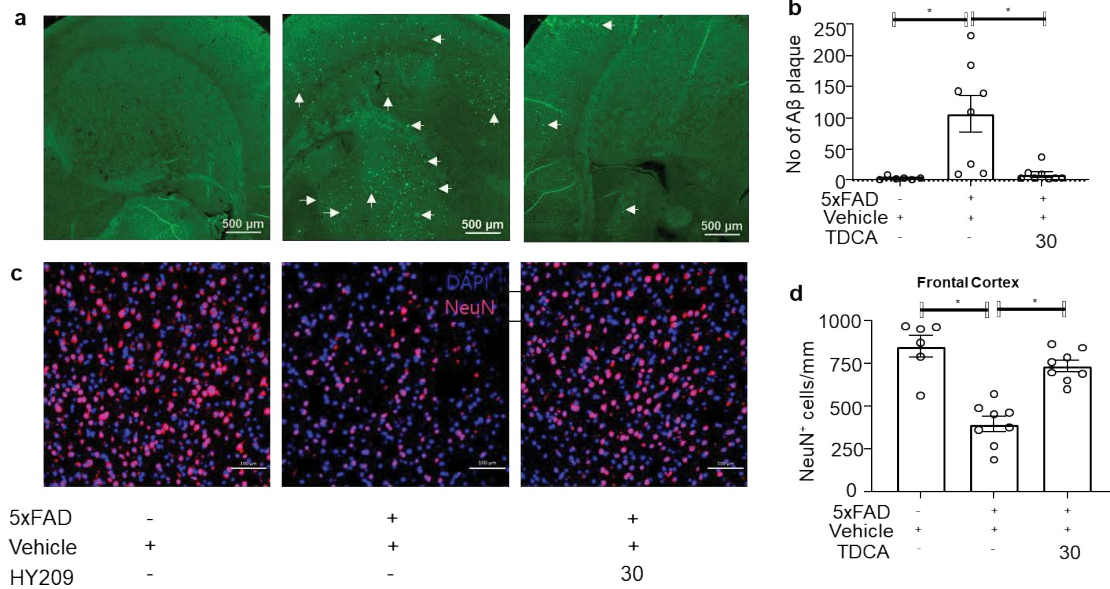


Figure 2: TDCA decreases A β plaque and increases NeuN+ cells in 5xFAD mice brain

5xFAD mice were treated with 30 mg/kg TDCA p.o. for 10 weeks. a, A β plaques in the brain paraffin sections were stained with Thioflavin-S (green dots indicated with white arrows, left panels). b, The number of plaques were quantitated using Image J. c, NeuN cells in the frontal cortex was analyzed using a confocal microscopy. The paraffin sections were made from the frontal cortex of the mice. A set of the representative images are depicted in the left panel, and d, the number of NeuN cells is shown in the right panel. The individual samples are shown with the mean \pm SEM and *P < 0.05 using Student's unpaired t-test throughout the study otherwise denoted.

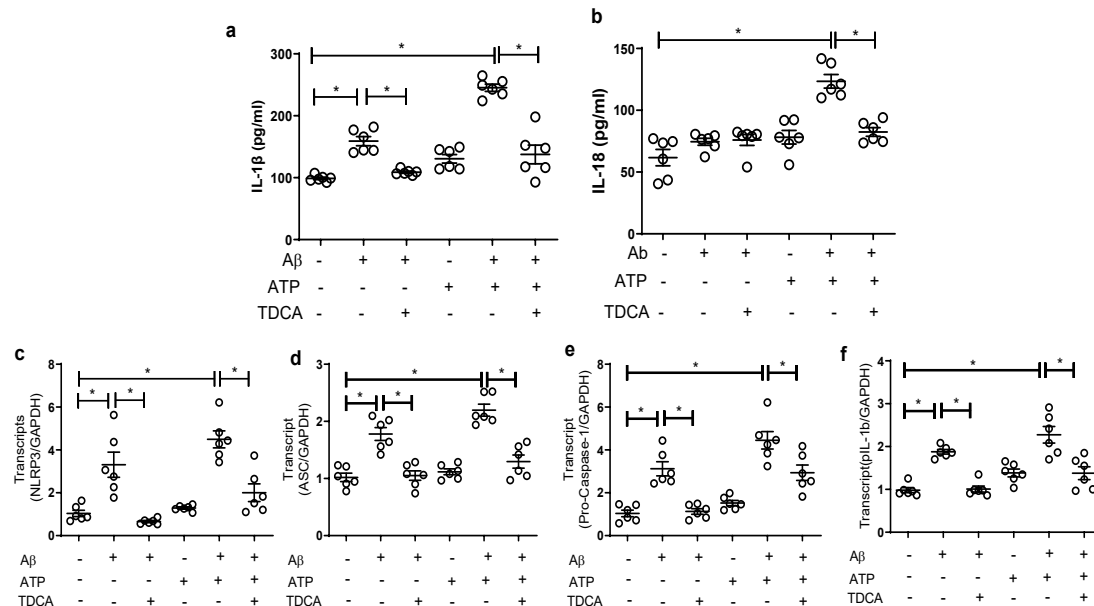


Figure 3: TDCA suppresses production of IL-1 β , IL-18 in microglia.

HMC3 Cells were incubated with A β oligomer (2 μ M) with or without TDCA (400ng/ml) for 24h with ATP (1mM) for an additional 1h. a, IL-1 β and b, IL-18 in the culture supernatants of HMC3 cells were analyzed using ELISA. Transcripts of c, NLRP3, d, ASC, e, pro-caspase-1, and f, IL-1 β in HMC3 cells were quantitated using qPCR after treatment with A β , TDCA, and ATP. Gene expression was normalized using GAPDH. The individual samples are shown with the mean \pm SEM and *P < 0.05 using Student's unpaired t-test throughout the study otherwise denoted.

In HMC3 microglial cells, Aβ treatment significantly increased the expression of NLRP3 and ASC (Figure 4a b and c). Treatment with Aβ + ATP does not further increase the expression of NLRP3 and ASC. TDCA treatment significantly suppressed the expression of these two molecules, as well as their colocalization (yellow dots, Figure 4d).

TDCA normalize expression of SRA suppressed by Aβ

HMC3 cells were cultured in presence or Aβ (2 μM) ± TDCA (400ng/ml) for different time point. Gene expression of SRA was highest in 24h after seeding the cells. Cells treated with Aβ (2 μM) failed to express SRA even after

72h of culture. Aβ mediated inflammation prevents normal microglial activity. Treatment with TDCA upregulates SRA gene expression and maxim expression was noted at 24h (Figure 5a). Different doses of TDCA were tested for SRA expression. At 24h, TDCA 400ng/ml shows maximum SRA expression in microglia (Figure 5b). Cell surface expression of SRA is critical for microglial phagocytic function which was measured by flow cytometry. TDCA also upregulates microglial surface SRA measured by flow cytometry (Figure 5c) and confocal microscopy (Figure 5d). The Mean Fluorescent Intensity (MFI) of SRA in TDCA with Aβ treated microglia shows higher compared to Aβ only treated microglia (Figure 5e).

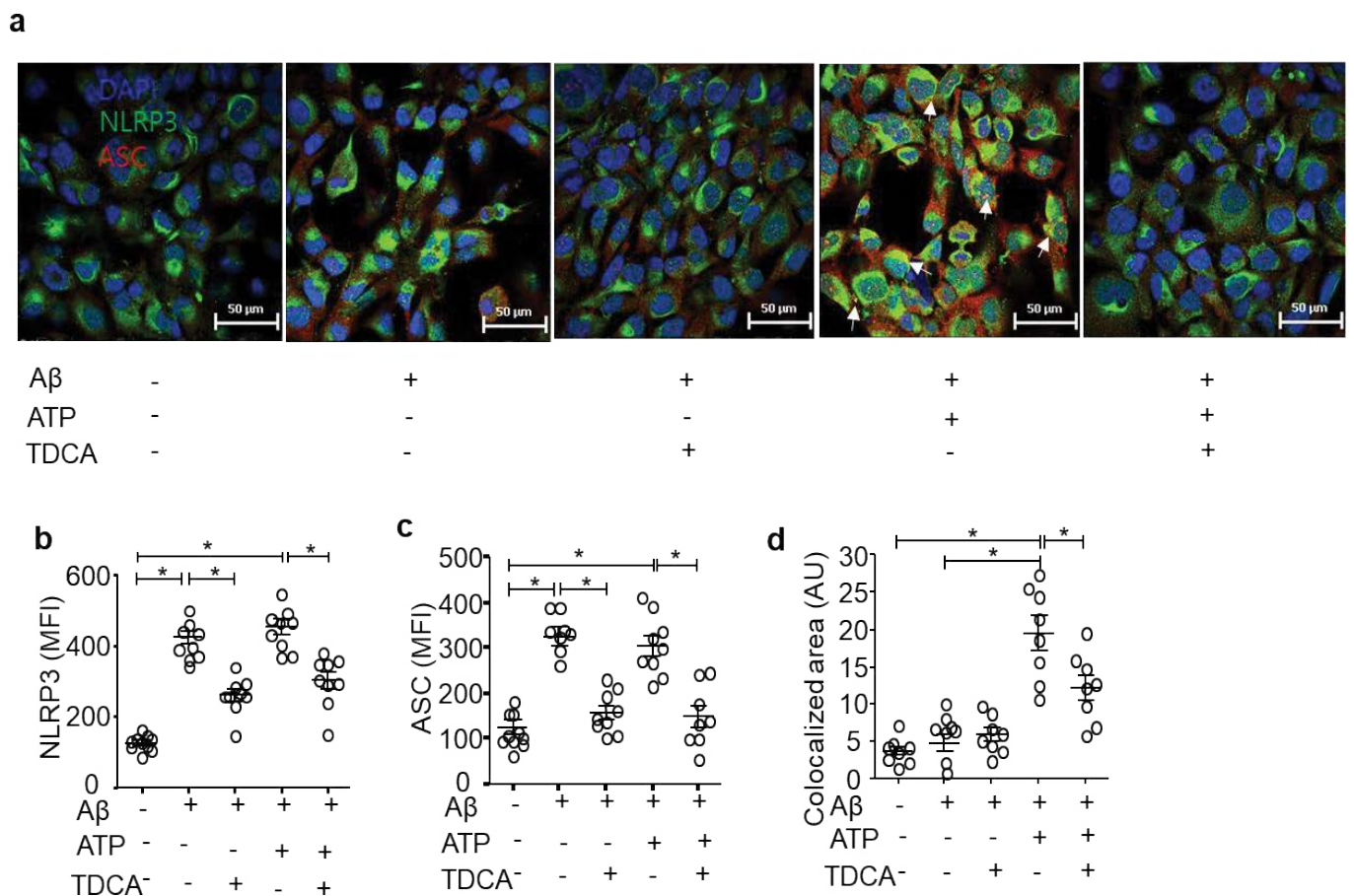


Figure 4: TDCA suppresses activation of the NLRP3 inflammasome in microglia.

HMC3 Cells were incubated with Aβ oligomer (2μM) with or without TDCA (400ng/ml) for 24h with ATP (1mM) for an additional 1h. a, The expression of NLRP3 (green) and ASC (red) was determined using confocal microscopy. Nuclei were stained with DAPI (blue). The mean fluorescent intensity (MFI) of b, NLRP3 and c, ASC expression was quantitated. d, Colocalization of NLRP3 and ASC (yellow) was analyzed using ImageJ. The individual samples are shown with the mean ± SEM and *P < 0.05 using Student’s unpaired t-test throughout the study otherwise denoted.

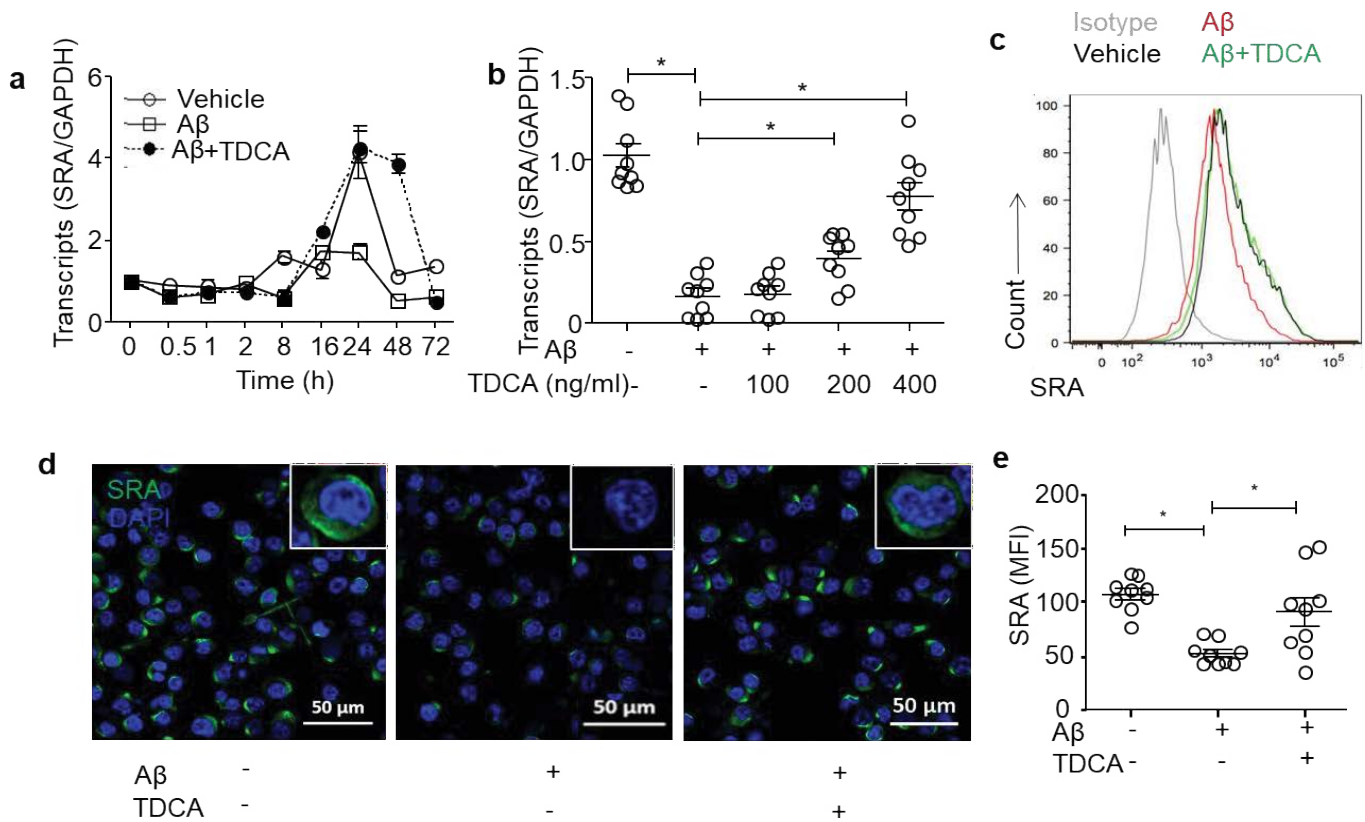


Figure 5: TDCA induces expression of scavenger receptor A expression in microglia.

Gene expression of SRA in HMC3 cells were quantitated using qPCR and normalized using GAPDH a, HMC3 Cells were incubated with Aβ oligomer (2μM) with or without TDCA (400ng/ml) for different time point until 72h. b, Different concentration of TDCA also tested for maximum expression of SRA with Aβ oligomer (2μM) treatment. d, The expression of SRA (green) was determined using confocal microscopy. Nuclei were stained with DAPI (blue). The mean fluorescent intensity (MFI) of e, SRA expression was quantitated. The individual samples are shown with the mean ± SEM and *P < 0.05 using Student's unpaired t-test throughout the study otherwise denoted.

Discussion

The findings of this study underscore the potential of taurodeoxycholic acid (TDCA) as a therapeutic agent for Alzheimer's disease (AD), particularly through its modulation of neuroinflammatory pathways and microglial function. Our results demonstrate that TDCA treatment significantly improves cognitive function in 5xFAD mice, a well-established model of familial AD, by enhancing spatial learning and memory (Figure 1). This cognitive enhancement is likely attributable to the reduction in amyloid-beta (Aβ) plaque burden, the suppression of neuroinflammation, and the promotion of neuronal survival, all of which were observed following TDCA administration (Figure 2 and 3).

The neuroprotective effects of TDCA appear to be mediated, at least in part, by its ability to inhibit the activation of the NLRP3 inflammasome in microglia. The NLRP3 inflammasome has been increasingly recognized as a critical player in the pathogenesis of AD, where its activation leads to the release of pro-inflammatory cytokines, such as IL-1β and IL-18, which exacerbate neuroinflammation and contribute to neuronal damage [23] [24] [13]. Our study confirms that TDCA effectively suppresses the expression

of key components of the NLRP3 inflammasome, including NLRP3 itself, ASC, and pro-caspase-1, in microglial cells treated with Aβ and ATP (Figure 3 c-f and Figure 4). This suppression correlates with a marked decrease in the secretion of IL-1β and IL-18 (Figure 3a and b), suggesting that TDCA exerts its anti-inflammatory effects by directly targeting this inflammasome pathway.

In addition to its effects on the NLRP3 inflammasome, TDCA also restores the expression of scavenger receptor A (SRA) in microglia, which is crucial for the clearance of Aβ. Aβ-induced inflammation is known to impair the normal phagocytic function of microglia, in part by downregulating SRA expression [25]. Our data show that TDCA not only prevents this

downregulation but also enhances SRA expression and its surface localization on microglia (Figure 5). This restoration of SRA expression likely contributes to the enhanced clearance of Aβ plaques observed in the brains of TDCA-treated 5xFAD mice, providing a dual mechanism by which TDCA may mitigate AD pathology: reducing neuroinflammation and promoting Aβ clearance.

The behavioral data from this study further supports the therapeutic potential of TDCA. The significant improvements in spatial learning and memory in TDCA-treated 5xFAD mice, as assessed by the Morris water maze and novel object recognition tests, highlight the compound's ability to translate its molecular and cellular effects into functional cognitive benefits (Figure 1). These findings are particularly encouraging, given that cognitive decline is the most debilitating symptom of AD, and current treatments offer limited efficacy in halting or reversing this aspect of the disease [26].

Moreover, the results indicate that TDCA offers a more accessible and less invasive treatment option compared to existing anti-amyloid therapies, such as aducanumab and lecanemab. These monoclonal antibodies, while effective in reducing A β plaques, are associated with significant challenges, including high costs, limited accessibility, and the need for intravenous administration [27]. In contrast, TDCA's oral administration, combined with its multifaceted effects on microglial function and A β clearance, positions it as a promising candidate for long-term management of AD.

Despite these promising findings, several limitations of the study should be acknowledged. Firstly, while the 5xFAD mouse model recapitulates key features of familial AD, it may not fully represent the complexity of sporadic AD in humans. Further studies in other AD models are necessary to validate the efficacy and safety of TDCA in a broader spectrum. Additionally, the long-term effects of TDCA treatment, including its potential impact, need to be investigated.

In conclusion, this study provides compelling evidence that TDCA has the potential to become a novel therapeutic agent for AD by targeting key neuroinflammatory pathways, enhancing microglial clearance of A β , and improving cognitive function. Given the central role of neuroinflammation in AD and other neurodegenerative diseases, TDCA's therapeutic effects may extend beyond AD, offering a broader application for treating chronic inflammatory conditions of the central nervous system. Further research is warranted to explore these possibilities and to determine the optimal dosing and administration regimens for TDCA in clinical settings.

Author Contributions

M. J. I. designed and conducted the experiments, wrote the manuscript as specified, and contributed to its preparation. J.-Y. K. and Y.-J. K. contributed to the studies involving the 5xFAD mouse model. S.-Y. S. conceived the study's concept and provided supervision throughout the research.

Conflict of Interest

The patent "Pharmaceutical composition for prevention, treatment, or delay of Alzheimer's disease or dementia containing G protein-coupled receptor 19 agent as active

ingredient: CN106794189, EP3248603, ES2750839, IN201747003504, JP2017523982, KR1020150095951, US20180104261" was invented by Seong et al. and applied by Seoul National University R&DB Foundation. The exclusive license for the patent was transferred from SNU R&DB to Shaperon Inc. S-YS is the founder of Shaperon Inc. and its current CEO.

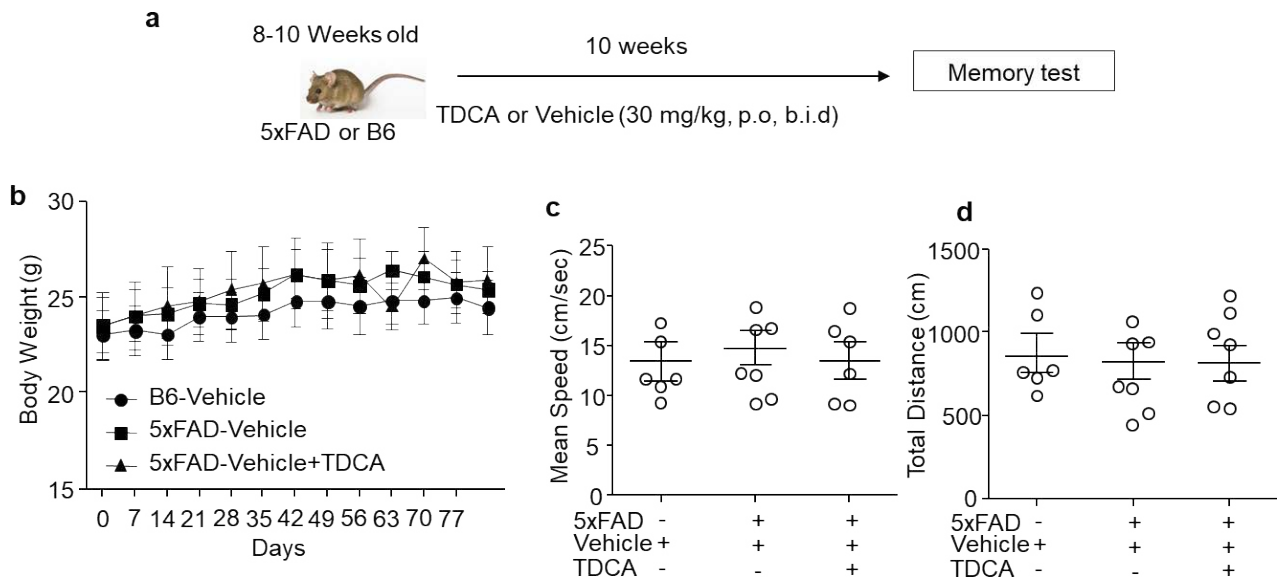
Funding

This work was supported by a grant funded by the National Research Foundation, Ministry of Science, ICT and future planning (2012R1A5A2A44671346); a grant from the Korea Healthcare Technology R&D Project, Ministry of Health and Welfare (A062260); a grant from Gangwon Province, Republic of Korea; a grant from Chemon Co., Ltd. (0654-20170002); a grant from Shaperon Inc. (0654-20200002); and a grant for Shaperon from the Ministry of Health and Welfare (HI19C0429).

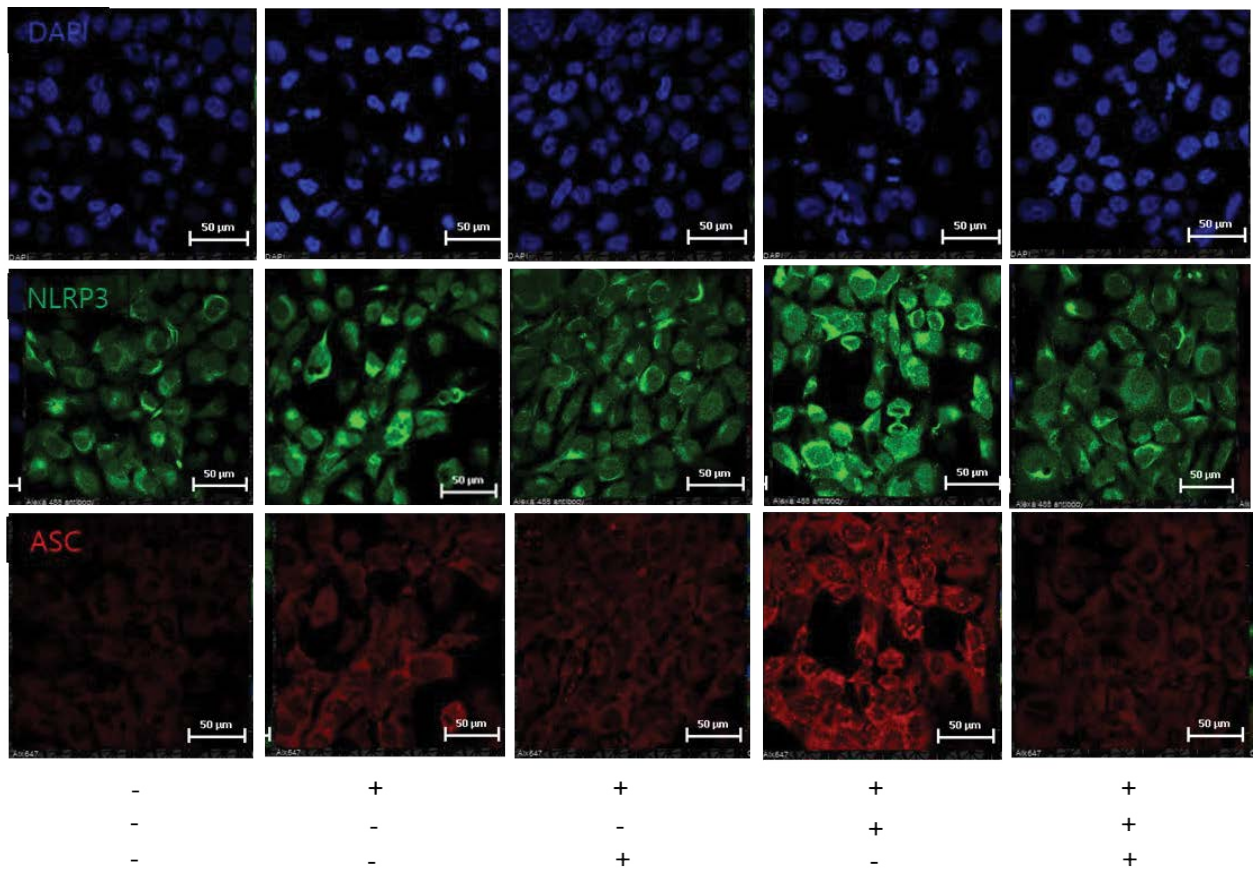
Références

1. DeTure MA, Dickson DW. The neuropathological diagnosis of Alzheimer's disease. *Molecular Neurodegeneration*, 14 (2019): 32.
2. Lieberman OJ, Lee S, Zabinski J. Donepezil treatment is associated with improved outcomes in critically ill dementia patients via a reduction in delirium. *Alzheimers Dement* 19 (2023): 1742-1751.
3. Olivares D. N-methyl D-aspartate (NMDA) receptor antagonists and memantine treatment for Alzheimer's disease, vascular dementia and Parkinson's disease. *Curr Alzheimer Res* 9 (2012): p. 746-758.
4. Singh B. Alzheimer's disease current therapies, novel drug delivery systems and future directions for better disease management. *Journal of Controlled Release* 367 (2024): p. 402-424.
5. Zhang Y. Amyloid β -based therapy for Alzheimer's disease: challenges, successes and future. *Signal Transduction and Targeted Therapy* 8 (2023): p. 248.
6. Dyck CHv. Lecanemab in Early Alzheimer's Disease. *New England Journal of Medicine* 388 (2023): p. 9-21.
7. Ameen Unraveling Alzheimer's: the promise of aducanumab, lecanemab, and donanemab. *The Egyptian Journal of Neurology, Psychiatry and Neurosurgery* 60 (2024): p. 72.
8. Liu P. Neuroinflammation as a Potential Therapeutic Target in Alzheimer's Disease. *Clin Interv Aging* 17 (2022): p. 665-674.
9. Gao C. Microglia in neurodegenerative diseases: mechanism and potential therapeutic targets. *Signal Transduction and Targeted Therapy* 8 (2023): p. 359.

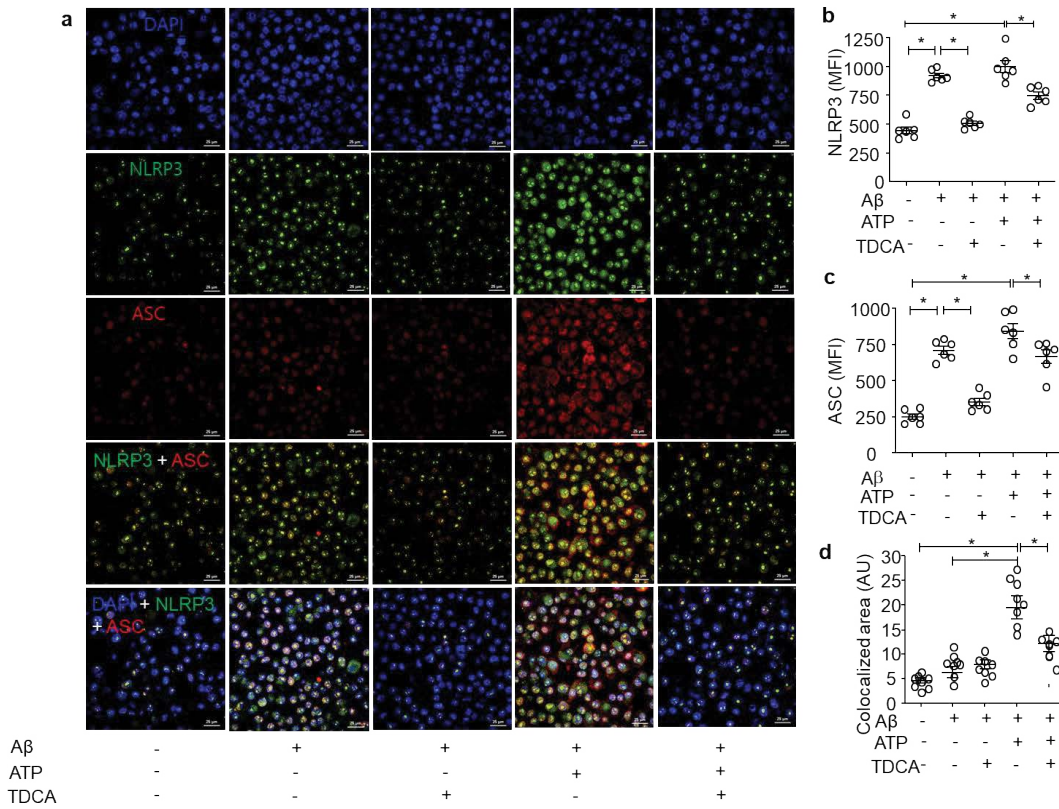
10. Lull ME, Block ML. Microglial Activation and Chronic Neurodegeneration. *Neurotherapeutics* 7 (2010): p. 354-365.
11. Yang Y. Recent advances in the mechanisms of NLRP3 inflammasome activation and its inhibitors. *Cell Death & Disease*, 2019. 10 (2019): 128.
12. Zhang Y, Dong Z, Song W. NLRP3 inflammasome as a novel therapeutic target for Alzheimer's disease. *Signal Transduction and Targeted Therapy* 5 (2020): p. 37.
13. Yao J. The role of inflammasomes in human diseases and their potential as therapeutic targets. *Signal Transduction and Targeted Therapy* 9 (2024): p. 10.
14. Ackerman HD and Gerhard GS. Bile Acids in Neurodegenerative Disorders. *Front Aging Neurosci* 8 (2016): p. 263.
15. Loh JS. Microbiota-gut-brain axis and its therapeutic applications in neurodegenerative diseases. *Signal Transduction and Targeted Therapy* 9 (2024): p. 37.
16. Islam J. GPCR19 Regulates P2X7R-Mediated NLRP3 Inflammasomal Activation of Microglia by Amyloid β in a Mouse Model of Alzheimer's Disease. *Front Immunol* 13 (2022): 766919.
17. Murakami T. Critical role for calcium mobilization in activation of the NLRP3 inflammasome. *Proceedings of the National Academy of Sciences*, 2012. 109 (2012): p. 11282-11287.
18. Rossol M. Extracellular Ca^{2+} is a danger signal activating the NLRP3 inflammasome through G protein-coupled calcium sensing receptors. *Nature Communications* 3 (2012): p. 1329.
19. Zhang H. Activated Scavenger Receptor A Promotes Glial Internalization of $\text{A}\beta$. *PLOS ONE*, 2014. 9 (2014): p. e94197.
20. Oakley H. Intraneuronal beta-amyloid aggregates, neurodegeneration, and neuron loss in transgenic mice with five familial Alzheimer's disease mutations: potential factors in amyloid plaque formation. *J Neurosci*, 2006. 26 (2006): p. 10129-10140.
21. Castel D. Open field and a behavior score in PNT model for neuropathic pain in pigs. *J Pain Res* 11 (2018): p. 2279-2293.
22. Parajuli B. Oligomeric amyloid beta induces IL-1beta processing via production of ROS: implication in Alzheimer's disease. *Cell Death Dis* 4 (2013): p. e975.
23. Liang T. The Role of NLRP3 Inflammasome in Alzheimer's Disease and Potential Therapeutic Targets. *Front Pharmacol* 13 (2022): p. 845185.
24. Ramachandran R. NLRP3 inflammasome: a key player in the pathogenesis of life-style disorders. *Experimental & Molecular Medicine* 56 (2024): p. 1488-1500.
25. Pan XD. Microglial phagocytosis induced by fibrillar β -amyloid is attenuated by oligomeric β -amyloid: implications for Alzheimer's disease. *Mol Neurodegener* 6 (2011): p. 45.
26. van der Flier WM. Towards a future where Alzheimer's disease pathology is stopped before the onset of dementia. *Nature Aging* 3 (2023): p. 494-505.
27. Brockmann, R. Impacts of FDA approval and Medicare restriction on anti-amyloid therapies for Alzheimer's disease: patient outcomes, healthcare costs, and drug development. *Lancet Reg Health Am* 20 (2023): p. 100467.



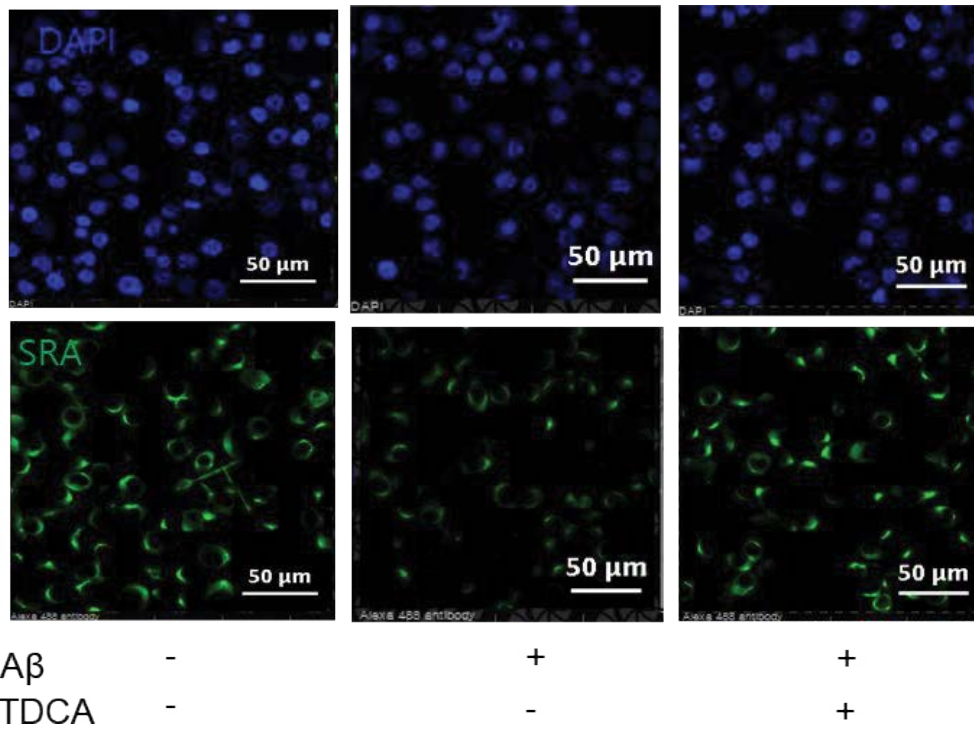
S Figure 1: a, A schematic diagram showing protocols of behavior test for 5xFAD and B6 mice after treatment with TDCA (30mg/kg) orally twice in a day for 10 weeks. b, Changes in the body weight of mice were depicted. c, Mouse mean speed and d, total distance during the probe test of MWM were compared between the groups of mice. The individual samples are shown with the mean \pm SEM and *P < 0.05 using Student's unpaired t-test.



S Figure 2: HMC3 microglia cells were treated with Aβ (2 μM), TDCA (400 ng/ml) for 24 h, and ATP (1 mM) for the last 1 h. Confocal microscopic slide of an individual channel for intracellular NLRP3 (green) and ASC (red) expression. The nuclei were stained with DAPI (blue).



S Figure 3: BV2 cells were treated with Aβ (2 μM), TDCA (400 ng/ml), and ATP (1 mM) for 1 h. Surface staining of cells showing NLRP3 (green) and ASC (red). The nuclei were stained with DAPI (blue). Merged NLRP3 (green) + ASC (red) channels show co-localization area (yellow). The mean fluorescent intensity (MFI) of b, NLRP3 c, ASC expression was quantitated. d, Colocalization of NLRP3 and ASC (yellow) was analyzed using ImageJ. The individual samples are shown with the mean ± SEM and *P < 0.05 using Student's unpaired t-test.



S Figure 4: HMC3 cells were treated with TDCA (400 ng/ml) and Aβ (2 μM) for 24h. Individual channel of confocal microscopy showing SRA (green). Nuclei were stained with DAPI (Blue).